Cathodoluminescence study of domains, defects, and interdiffusion in ZnSe/GaAs(100)

H. T. Lin, D. H. Rich,[a] and D. B. Wittry
Department of Materials Science and Engineering, University of Southern California, Los Angeles, California 90089-0241

(Received 12 November 1993; accepted for publication 7 March 1994)

The distribution of dislocations and domains found in thin ZnSe films grown by molecular-beam epitaxy on GaAs(100) has been examined with low-temperature cathodoluminescence (CL) imaging and spectroscopy. Dark-line and bright-line defects in the low-temperature CL imaging of the free-exciton (FE) and Y-band emissions, respectively, are found to correlate with the presence of $[1\bar{1}0]$-oriented misfit dislocations for 1-μm-thick films found to grow nearly two dimensionally. For a sample exhibiting mixed two- and three-dimensional growth characters, large domains ($\sim$1–5 μm widths) in the CL imaging of the ZnSe FE emission were found to correlate with a cellular pattern found in the imaging of the GaAs exciton and band-edge–to–acceptor emissions. These results show that the optical properties of the ZnSe film and GaAs substrate are coupled and influenced by Zn diffusion into the substrate during growth.

I. INTRODUCTION

ZnSe, one of the most promising II-VI wide band-gap semiconductor materials, has attracted a great deal of attention in the blue wavelength range for optoelectronic device applications. The potential for hybridization of II-VI with III-V optoelectronics has led to significant efforts in optimizing the epitaxial growth of ZnSe layers on GaAs substrates.[1,2] The residual strain, attributed to both lattice mismatch (0.27% between ZnSe and GaAs at room temperature) and different thermal-expansion coefficients, results in structural defects such as dislocations, stacking faults, and microtwins.[2] In addition, both intrinsic and extrinsic background defects, such as vacancies and unintentional impurities, can be introduced during the heteroepitaxial growth.[1] More comprehensive studies should also examine the influence of ZnSe growth on the structural and optical properties of the GaAs substrates since device performance may depend on the quality and stability of the interfacial region. A variety of analysis techniques including photoluminescence (PL),[1–4] x-ray diffraction,[2] and transmission electron microscopy (TEM)[2,3] has been used to characterize the optical and structural quality of ZnSe films.

We have studied the interplay between the structural and optical properties of ZnSe/GaAs(100) using low-temperature cathodoluminescence (CL) imaging and spectroscopy. In particular, the influence of the mode of growth on the resulting optical properties has been examined. Using molecular-beam epitaxy (MBE) for the growth of lattice-mismatched heterostructures, the growth modes of ZnSe/GaAs(100) can be varied between two-dimensional (2D) layer-by-layer and the Volmer–Weber type in which three-dimensional (3D) islands nucleate and grow during the initial stages of interface formation.[2] Guha and co-workers,[2] using TEM, have shown that the dislocation distribution in ZnSe/GaAs films is affected by the formation of 3D islands which cause a marked enhancement in the threading dislocation density and shortening of the misfit dislocation segment length. Using CL, we have established, for the first time, a correlation between the commonly observed Y bands seen in photoluminescence of ZnSe/GaAs with the presence of $[1\bar{1}0]$-oriented misfit dislocations. We also address the modification of the GaAs substrate optical properties, and find a correlation between the occurrence of domains in the ZnSe film and the presence of enhanced Zn acceptor incorporation at cellular boundaries in the GaAs substrate. The interdiffusion of Zn and Ga at the ZnSe-to-GaAs interface for MBE-grown samples was recently found to affect the heterojunction band bending near the interface and to influence carrier transport.[5] Therefore, an understanding of the interplay between the electronic, optical and structural properties of ZnSe films and the host GaAs substrates is of paramount importance in assessing the feasibility for hybrid device fabrication.

II. EXPERIMENT

The MBE growth procedure for the ZnSe/GaAs(100) samples studied here has been previously described.[2] Different growth conditions were employed to achieve the 2D layer-by-layer and 3D growth modes. Briefly, an As-stabilized GaAs(100)-(2×1) surface at 300 °C was exposed to both Zn and Se fluxes simultaneously and resulted in mixed 2D and 3D growth characters, previously referred to as an intermediate 2D (I2D) mode,[2] as determined from a reflection high-energy electron-diffraction (RHEED) analysis. When the As-stabilized GaAs(100)-(2×1) surface at 300 °C was exposed to a Zn flux for about 1 min prior to exposure to the Se flux, RHEED analysis showed the growth to be a nearly ideal 2D layer by layer. The I2D- and 2D-type ZnSe films were grown to thicknesses of 2700 Å and 1.0 μm, respectively. Subsequent TEM analysis of the I2D sample showed that the misfit dislocations are mainly 60° dislocations with segment lengths less than $\sim$1 μm and a threading dislocation density of about 3×10^8 cm^{-2}. The TEM analysis of the 2D sample showed a threading dislocation density of $\sim1\times10^6$ cm^{-2}. X-ray-diffraction measure-

[a]Author to whom correspondence should be addressed.

 0021-8979/94/75(12)/8080/5/$6.00

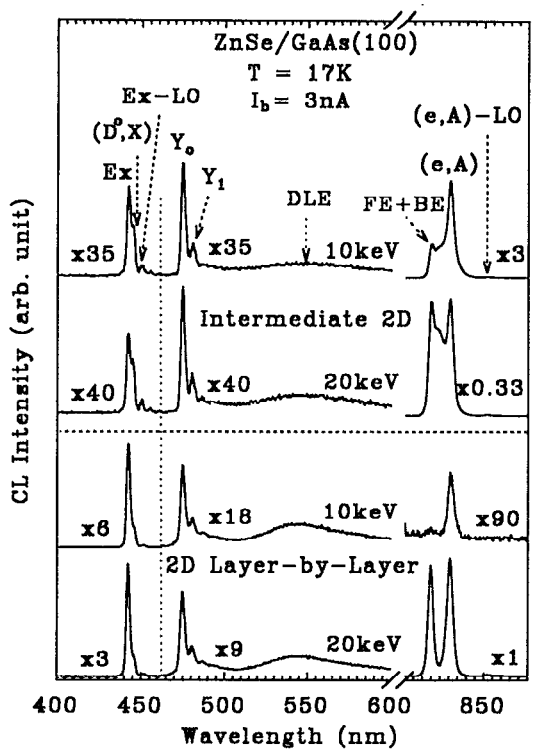

FIG. 1. CL spectra of ZnSe/GaAs(100) exhibiting 2D layer-by-layer and I2D modes. Spectra taken with 10 and 20 keV electron-beam energies are shown.

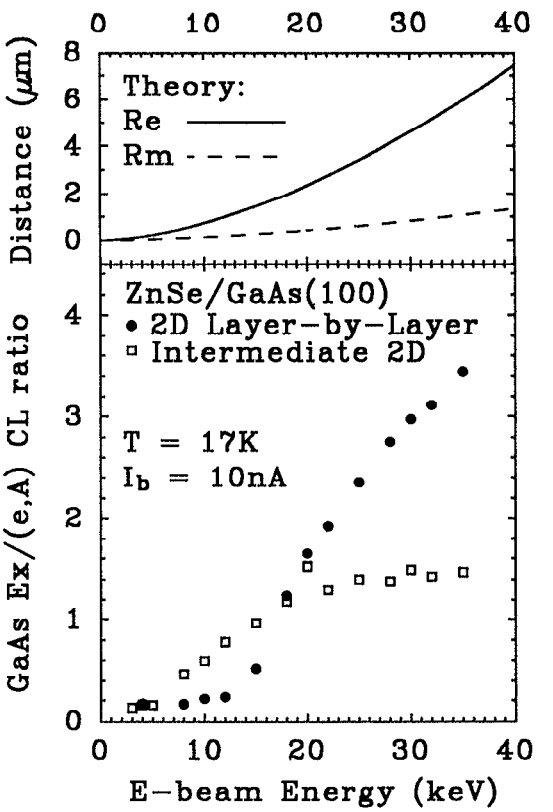

FIG. 2. GaAs FE+BE to (e,A) CL intensity ratio vs electron-beam energy. Results for the 2D and I2D samples are shown for $T=17$ K and a fixed beam current of 10 nA. Theoretical plots, based on the model of Everhart and Hoff (in Ref. 7), for the one-dimensional electron-hole pair density maximum peak position R_m and the electron penetration range R_e as a function of electron beam energy are shown at the top of the figure.

ments of the I2D and 2D samples indicated that about 30% and 75%, respectively, of the elastic strain had been relieved.

Cathodoluminescence measurements were performed with a JEOL 840-A scanning electron microscope. The CL optical collection system and low-temperature cryogenic specimen stage were designed and constructed at USC. The luminescence emitted from the sample was collected with an ellipsoidal mirror which focuses the radiation onto an optical fiber bundle leading outside the SEM vacuum chamber to a 0.25 m focal length monochromator which was set for a 1 nm total spectral resolution. A cooled GaAs:Cs photomultiplier photon counting system was used for detection.

III. CL RESULTS AND DISCUSSION

A. CL spectra of ZnSe/GaAs 2D and I2D samples

Cathodoluminescence spectra of the 2D and I2D samples are shown in Fig. 1. A beam current of 3 nA rastered over a 120×90 μm^2 region of the samples was used. The samples were maintained at a temperature of ~17 K. The electron-beam energy was varied and spectra for 10 and 20 keV beam energies for each sample are shown. The relative scaling factors for each portion of the spectra are indicated. The samples show sharp emission peaks associated with the free exciton E_x, at a wavelength of 443 nm and its LO phonon replica, E_x-LO, at 450 nm.[3] Also, appearing as a shoulder on the lower-energy side of E_x are emissions stemming from the donor-bound exciton (D^0,X) at 445 nm, where the donor is most likely Ga on Zn sites.[1-4] Emissions labeled Y_0 and Y_1 are observed in the spectra. These have previously been attributed to the presence of structural defects from PL and TEM studies.[3] A broad deep-level emission (DLE) peak associated with impurities or defects is centered at 545 nm.[1] Because the band gap of the ZnSe film is greater than that of GaAs, the optical properties of the GaAs film can easily be studied by tuning the electron-beam energy so that significant electron-hole pair creation takes place in the substrate.[6,7] The GaAs near-band-edge emission features are readily observed with the free-exciton (FE) and bound-exciton (BE) emissions observed at 820 nm. The intense peak at 831 nm is associated with the free-electron–to–acceptor transition (e,A).[8,9] The incorporation of Zn into the GaAs interfacial region during the MBE growth is expected to give rise to this emission, and a previous study of Zn-ion-implanted GaAs corroborates with this emission energy.[9] The presence of carbon impurities in the bulk GaAs would also be expected to give rise to a similar emission energy.[8,9]

In order to distinguish between Zn and C, we have examined the GaAs near-band-edge CL spectra for different electron-beam energies; spectra for 10 and 20 keV are shown in Fig. 1. The ratio of GaAs FE+BE and (e,A) peak CL intensities versus electron beam energy for both 2D and I2D samples is shown in Fig. 2. A variation in the beam energy over the range 10–40 keV results in a corresponding tenfold increase in the penetration depth R_e, and the peak position

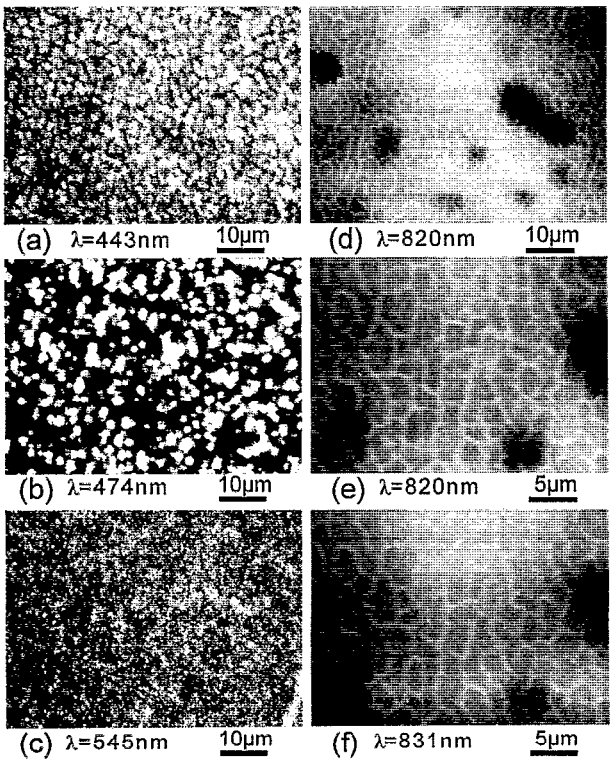

FIG. 3. Monochromatic CL images taken with a 17 K sample temperature, 20 keV beam energy, and 3 nA beam current for the ZnSe/GaAs(100) sample exhibiting intermediate 2D growth.

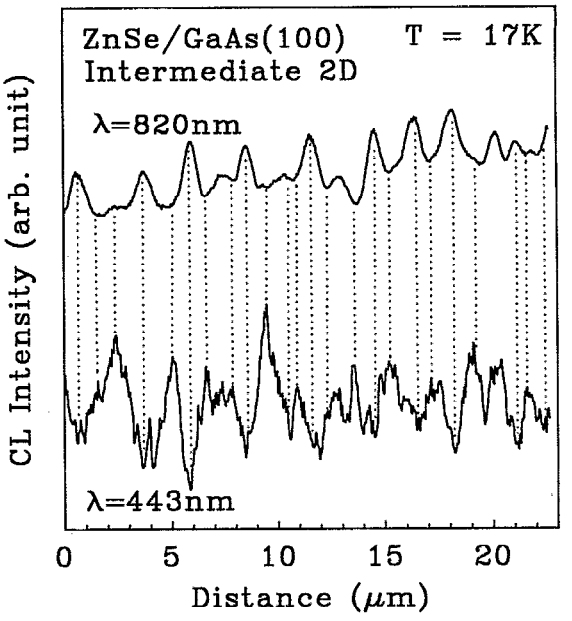

FIG. 4. CL line scan (intensity vs distance histogram at a 20 keV beam energy and 3 nA beam current) of the intermediate 2D sample showing the spatial correlation of the ZnSe free exciton at domain boundaries and GaAs substrate emissions in the cellular structure.

R_m, of the electron-hole pair density creation function.[6,7] Theoretical plots of R_m and R_e as a function of the beam energy, from the one-dimensional penetration model of Everhart and Hoff,[7] are shown at the top of Fig. 2 for an electron-beam excitation in GaAs. It is apparent that by probing deeper into the sample, with higher-energy beams,[6,7] the ratio of the FE+BE to (e,A) emission intensity increases markedly for both 2D and I2D samples, demonstrating that acceptor incorporation occurs at the ZnSe-to-GaAs interface, where the Zn concentration is expected to be the greatest. Also, the marked increase in the Fe+Be to (e,A) emission ratio for energies greater than 5 and 12 keV, corresponding to an R_e of 0.23 and 1.0 μm (as shown in Fig. 2), demonstrates that electron-hole pair generation in the GaAs region below the interface begins at ~5 and ~12 keV for the I2D and 2D samples, which have ZnSe film thicknesses of 0.27 and 1.0 μm, respectively. Therefore, the electron-beam energies at which there is an onset of an enhanced FE+BE emission relative to (e,A) emission correspond to probing depths which correlate strongly with the positions of the ZnSe/GaAs interfaces for both 2D and I2D samples, showing that Zn is incorporated into the GaAs at the interface during ZnSe growth, in agreement with Ref. 5.

B. Monochromatic CL imaging of I2D ZnSe/GaAs

Scanning monochromatic CL images for the I2D sample are presented in Fig. 3. The images in Figs. 3(a)–3(d) and Figs. 3(e) and 3(f) are over the same regions, respectively, and thus facilitate a spatial comparison of the various emissions. Figure 3(a) shows a CL image with λ=443 nm, corresponding to the FE emission. The image reveals bright spots having less than ~5 μm width surrounded by well-defined dark boundaries having a reduced radiative recombination efficiency. The CL image corresponding to the Y_0 emission at 474 nm is shown in Fig. 3(b). Regions of high Y_0 emission intensity are surrounded by larger dark regions. The Y_0 emission has been previously attributed to the presence of dislocations,[3] although the spatial distribution was not studied. Therefore, in Fig. 3(b), the bright regions are associated with the Y_0 emission and must delineate regions of higher dislocation density relative to adjacent darker regions in the image. Figure 3(c) shows the DLE distribution at 545 nm which is spread nearly homogeneously in the image. Figure 3(d) is an image of the GaAs FE+BE emission at 820 nm. The image of Fig. 3(f) is of the (e,A) emission at 831 nm. These images reveal a well-defined cellular pattern which reflects the complex morphology of domain formation during ZnSe growth. Figures 3(e) and 3(f) are of the GaAs FE+BE and (e,A) emissions which reveal a nearly identical cellular pattern. The results indicate that an enhanced Zn acceptor incorporation occurs at the cell boundaries thereby giving rise to an enhanced luminescence.

Figure 4 shows an intensity versus position histogram for an arbitrary line scan at the ZnSe FE (443 nm) and GaAs FE+BE (820 nm) emissions. There is a clear spatial correlation between the peaks and valleys in the luminescence, indicating that the ZnSe FE emission is associated with emission from the center of domains while the cellular structure of Fig. 3(d) is associated with domain boundaries. For the case of $In_xGa_{1-x}As/GaAs(100)$ grown for compositions that led to three-dimensional island growth, Ghaisas and Madhukar[10] argued that defects and dislocations can form as

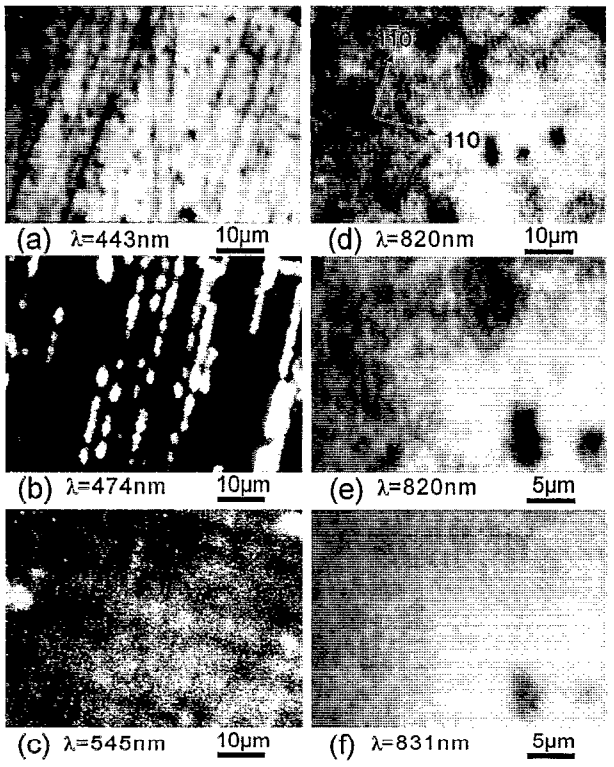

FIG. 5. Monochromatic CL images taken with a 17 K sample temperature, 20 keV beam energy, and 3 nA beam current for the ZnSe/GaAs(100) sample exhibiting 2D layer-by-layer growth.

a result of the coalescence of 3D islands. Therefore, it is our hypothesis that coalescence of islands in ZnSe/GaAs(100) can lead to the presence of cellular boundaries. These boundaries are characterized by a relatively high defect concentration which decreases the recombination efficiency for ZnSe FE emission. This reduction in recombination efficiency at the cell boundaries is consistent with the observed dark regions surrounding bright spots in Fig. 3(a). In support of this view, a previous CL study of polycrystalline ZnSe has shown the quenching of bandedge luminescence at the grain boundaries.[11] Likewise, the enhanced Zn doping in the GaAs at the domain or cell boundary could result from high-diffusivity Zn pathways to the GaAs substrate resulting from threading dislocations and subgrain boundaries.[12] These enhanced regions of Zn incorporation in the GaAs substrate would lead to a cellular pattern, as measured in Fig. 3(d), that would mirror the boundaries generated by ZnSe island coalescence which is indicated by the regions of reduced radiative recombination efficiency in Fig. 3(a). The increase in the GaAs FE+BE to (e,A) emission intensity ratio (Figs. 1 and 2) as the probing depth is increased also further supports the notion that the Zn acceptors are diffusing into GaAs from high-concentration sources along the ZnSe-to-GaAs interface.

C. Monochromatic CL imaging of 2D ZnSe/GaAs

Cathodoluminescence imaging of the 2D layer-by-layer sample is illustrated in Fig. 5. Figure 5(a) is the ZnSe FE emission image at 443 nm. Dark-line defects (DLDs) and dark spots, as a result of misfit and threading dislocations, respectively, are seen. The CL imaging of the InGaAs/GaAs system also shows misfit-dislocation-induced DLDs occurring almost exclusively along the high-symmetry [110] and [1$\bar{1}$0] directions.[13] The image of Fig. 5(a), however, shows DLDs occurring along [110], [1$\bar{1}$0], and at intermediate angles off these high-symmetry axes. Previous TEM measurements have shown that the off-axis dislocations are actually comprised of "zig-zag" segments of [110]- and [1$\bar{1}$0]-oriented 60°-type misfit dislocations.[2] These segments are short (less than ~100 nm), and would not be observable in CL imaging as a result of the ~1 μm resolution resulting from the electron-beam-induced excitation volume at 20 keV convolved with the ~0.1 μm minority-carrier diffusion length in ZnSe. The CL image of the Y_0 emission (474 nm) is shown in Fig. 5(b). The image shows bright-line defects (BLDs) oriented primarily along [1$\bar{1}$0]. The absence of BLDs along the other directions suggests an anisotropy in the electronic properties of [110]- and [1$\bar{1}$0]-oriented 60°-type misfit dislocations. The cores of 60° misfit dislocations oriented along [110] and [1$\bar{1}$0] will have extra half-planes in the substrate which terminate with either Ga (α type) or As (β type) atoms, thereby exhibiting different electronic and structural properties.[14] Thus, the anisotropy in Y_0 emission that gives rise to BLDs exclusively along [1$\bar{1}$0] in Fig. 5(b) may result from structural differences between α and β cores. The CL image of DLE (at 545 nm) is shown in Fig. 5(c). The influence of dislocations can be seen along both ⟨110⟩ directions, as faint DLDs are observed as a result of competition between recombination channels.

Figures 5(d), 5(e), and 5(f) are CL images of the GaAs substrate emissions at the wavelengths shown. Long wavy bright streaks ~1 μm in width are observed in Figs. 5(d)–5(f). The spatial correlation of the images of Figs. 5(e) and 5(f), like those of Figs. 3(e) and 3(f) for the I2D sample, shows that the local variation in emission intensity is related to variations in Zn acceptor incorporation. The differences in the emission patterns of Figs. 3(e) and 5(e) further demonstrate that complex pathways for Zn diffusion (e.g., possibly via surface defects such as missing As-dimer vacancies, kinks, and surface steps on the clean GaAs substrate prior to ZnSe growth)[15] into GaAs are connected to the mode of ZnSe growth.

IV. CONCLUSION

In conclusion, we have examined the optical properties of ZnSe/GaAs(100) using different MBE growth procedures which lead to intermediate 2D and 2D layer-by-layer growth modes. After analyzing the GaAs exciton- and acceptor-derived CL emissions as a function of electron-beam probing depth, we conclude that Zn-acceptor diffusion into GaAs occurs at the ZnSe/GaAs interface. Likewise, CL emission derived from the donor-bound exciton, which most likely originates from Ga diffusion into the ZnSe epilayer, is measured. For intermediate 2D growth, an enhanced Zn incorporation into GaAs is found to occur at ZnSe domain boundaries, as a cellular pattern was observed in the monochromatic CL imaging of the GaAs substrate emissions. Layer-by-layer growth results in strain relief via the formation of long misfit

dislocation segments which correlate with the Y_0 emission, appearing as bright-line defects in the CL image, along only one of the ⟨110⟩ directions. The present study demonstrates that interdiffusion between elements originating from the substrate and epilayer which in our case is Ga and Zn, respectively, can be monitored by simultaneously performing measurements of CL emissions that stem from both the film and substrate.

ACKNOWLEDGMENTS

We would like to thank Dr. Hiro Munekata of IBM, T. J. Watson Research Center, in whose laboratory the samples were grown, and Dr. Supratik Guha of 3M Corporate Research Labs for useful discussions. This work was supported by grants from the Charles Lee Powell Foundation and by the National Science Foundation under Grant No. DRM-9123568.

[1] J. Gutowski, N. Presser, and G. Kudlek, Phys. Status Solidi A **120**, 11 (1990).
[2] S. Guha, H. Munekata, and L. L. Chang, J. Appl. Phys. **73**, 2294 (1993); Appl. Phys. Lett. **60**, 3220 (1992).
[3] K. Shahzad, J. Petruzzello, D. J. Olego, D. A. Cammack, and J. M. Gaines, Appl. Phys. Lett. **57**, 2452 (1990).
[4] K. Shahzad, D. J. Olego, and D. A. Cammack, Phys. Rev. B **39**, 13 016 (1989).
[5] L. Kassel, J. W. Garland, P. M. Raccah, M. A. Haase, and H. Cheng, Semicond. Sci. Technol. **6**, A146 (1991); Appl. Phys. Lett. **56**, 42 (1990).
[6] D. B. Wittry and D. F. Kyser, J. Appl. Phys. **38**, 375 (1967).
[7] T. E. Everhart and P. H. Hoff, J. Appl. Phys. **42**, 5837 (1971).
[8] S. Shigetomi, Y. Makita, A. C. Beye, A. Yamada, N. Ohnishi, and T. Matsumori, J. Appl. Phys. **69**, 1631 (1991).
[9] N. Ohnishi, Y. Makita, K. Irie, K. Kudo, T. Nomura, H. Tanaka, M. Mori, and Y. Mitsuhashi, J. Appl. Phys. **60**, 2502 (1986).
[10] S. V. Ghaisas and A. Madhukar, J. Vac. Sci. Technol. B **7**, 264 (1989).
[11] G. J. Russell, P. Waite, and J. Woods, in *Microscopy of Semiconducting Materials*, Oxford, Inst. Phys. Conf. Ser. No. 60 (IOP, London, 1981), p. 371.
[12] P. Shewmon, *Diffusion in Solids* (The Minerals, Metals, and Materials Society, Warrendale, PA, 1989), Chap. 6.
[13] D. H. Rich, T. George, W. T. Pike, J. Maserjian, F. J. Grunthaner, and A. Larsson, J. Appl. Phys. **72**, 5834 (1992).
[14] M. S. Abrahams, J. Blanc, and C. J. Buiocchi, Appl. Phys. Lett. **21**, 185 (1972).
[15] M. D. Pashley, K. W. Haberern, and J. M. Gaines, Appl. Phys. Lett. **58**, 406 (1991).